Editors' Suggestion

Quench Dynamics of Collective Modes in Fractional Quantum Hall Bilayers

Zhao Liu,[1] Ajit C. Balram,[2] Zlatko Papić,[3] and Andrey Gromov[4]
[1]Zhejiang Institute of Modern Physics, Zhejiang University, Hangzhou 310027, China
[2]Institute of Mathematical Sciences, HBNI, CIT Campus, Chennai 600113, India
[3]School of Physics and Astronomy, University of Leeds, Leeds LS2 9JT, United Kingdom
[4]Brown Theoretical Physics Center and Department of Physics, Brown University, 182 Hope Street, Providence, Rhode Island 02912, USA

(Received 12 November 2020; accepted 22 January 2021; published 19 February 2021)

We introduce different types of quenches to probe the nonequilibrium dynamics and multiple collective modes of bilayer fractional quantum Hall states. We show that applying an electric field in one layer induces oscillations of a spin-1 degree of freedom, whose frequency matches the long-wavelength limit of the dipole mode. On the other hand, oscillations of the long-wavelength limit of the quadrupole mode, i.e., the spin-2 graviton, as well as the combination of two spin-1 states, can be activated by a sudden change of band mass anisotropy. We construct an effective field theory to describe the quench dynamics of these collective modes. In particular, we derive the dynamics for both the spin-2 and the spin-1 states and demonstrate their excellent agreement with numerics.

DOI: 10.1103/PhysRevLett.126.076604

Introduction.—A paradigmatic property of condensed phases of matter is the existence of a collective mode—coherent oscillations of the medium—which governs the system's low-energy physics [1]. The Feynman-Bijl ansatz [2] or "single-mode approximation" (SMA) is an elegant formulation of this idea, originally applied to understand the emergent phonon and roton excitations in liquid helium. The same idea has found applications in correlated systems, such as the plasmon modes in three-dimensional (3D) electron systems [3,4] and 1D quantum spin systems [5–11]. Recent progress in tensor networks has enabled accurate descriptions of collective modes in both 1D and 2D lattice systems [12,13].

Collective excitations are also ubiquitous in strongly correlated topological phases in two-dimensional electron gases (2DEGs), which are experimentally observed in the regime of the fractional quantum Hall (FQH) effect [14]. While there has been much focus on understanding the properties of *charged* excitations of FQH phases, fueled by their exotic properties such as fractional charge and fractional statistics [15–17], recently there has been a resurgence of interest in the *neutral* collective modes of FQH systems, some of which are also accurately described using the SMA [18–22]. In comparison with 1D or topologically trivial systems, the FQH collective modes are endowed with additional physical properties, which makes their physics much richer. For example, it has recently been realized that the long-wavelength limit of the SMA excitation, called the Girvin-MacDonald-Platzman (GMP) mode [18,19] exhibits an emergent quantum geometry [23–25]. This geometric degree of freedom has been dubbed FQH "graviton" since it carries angular momentum $L = 2$, reminiscent of the spin-2 elementary particle [21,24,26,27]. The conventional probes of FQH collective modes by inelastic light scattering [28–31] are limited to finite momenta k, thus they can only indirectly measure the graviton which emerges in $k \to 0$ limit. In contrast, recent works in single-layer FQH systems [32,33] have shown that the graviton can be directly excited in a dynamical quench experiment, where the band mass tensor of the 2DEG is suddenly made anisotropic or the magnetic field is abruptly tilted (see also a recent proposal using surface acoustic waves [34]).

Despite this progress in understanding the dynamics of the collective mode in single-layer FQH systems, many interesting new questions arise in multicomponent FQH systems [35], such as FQH bilayers. The additional layer degree of freedom gives rise to *multiple* collective excitations [20,36–38], thereby presenting a new avenue to study the nonequilibrium dynamics of FQH systems. In this Letter, we show that FQH bilayers provide a versatile platform to probe the dynamics of individual or coupled collective modes with rich topological and geometric properties. We report the investigation of an FQH bilayer system of bosons at total filling $\nu = 2/3$, which hosts two collective modes: a spin-2 excitation (graviton or quadrupole) and a spin-1 (dipole) excitation. We design two types of quench protocols corresponding to the change of mass tensor and the application of an electric field, which are shown to excite either the individual modes or their combination. We support these findings using extensive exact diagonalization calculations of the real-time evolution of the FQH bilayer system and formulating a field-theoretic description of the quench.

Model.—We consider a bilayer FQH system at total filling $\nu = 2/3$ on the square torus with N bosons and $N_\phi = N/\nu$ magnetic flux quanta. We label the two layers by $\sigma = \uparrow, \downarrow$, and neglect interlayer tunneling. Hence, the number of bosons in each layer N^σ is conserved and we focus on the density-balanced case with pseudospin $S_z \equiv \frac{1}{2}(N^\uparrow - N^\downarrow) = 0$. We assume that the bosons reside in the lowest Landau level (LLL), and their interaction is described by the Hamiltonian

$$H = \sum_{\mathbf{q}} \sum_{\sigma,\sigma'=\uparrow,\downarrow} \bar{V}_{\mathbf{q}}^{\sigma,\sigma'} : \rho_{\mathbf{q}}^{\sigma} \rho_{-\mathbf{q}}^{\sigma'} : . \tag{1}$$

Here, $\rho_{\mathbf{q}}^{\sigma} = \sum_{j=1}^{N^\sigma} e^{i\mathbf{q}\cdot\mathbf{R}_j^\sigma}$ is the LLL-projected density operator in layer σ, with $\mathbf{R}_j^\sigma$ the jth particle's guiding center coordinate [39], $\bar{V}_{\mathbf{q}}^{\sigma,\sigma'}$ is the Fourier transform of the interaction, and : : denotes normal ordering.

The Fourier transform of the interaction is a product of the Coulomb potential and the LLL form factors, $\bar{V}_{\mathbf{q}}^{\sigma,\sigma'} = V_{\mathbf{q}}^{\sigma,\sigma'} F_{\mathbf{q}}^{\sigma} F_{\mathbf{q}}^{\sigma'}$. The intralayer potentials are $V_{\mathbf{q}}^{\uparrow\uparrow} = V_{\mathbf{q}}^{\downarrow\downarrow} = 2\pi/|\mathbf{q}|$, and the interlayer interaction is $V_{\mathbf{q}}^{\uparrow\downarrow} = (V_{\mathbf{q}}^{\downarrow\uparrow})^* = (2\pi/|\mathbf{q}|)e^{-|\mathbf{q}|d} e^{i\mathbf{q}\cdot\mathbf{s}}$, where d is the interlayer distance, and $\mathbf{s} = (s_x, s_y)$ is the interlayer displacement between bosons in different layers. Throughout this work we quote energies in units of $e^2/(\varepsilon \ell_B)$, where the magnetic length $\ell_B = \sqrt{\hbar c/(eB)}$ and ε is the dielectric constant of the host material. The quantity d/ℓ_B can be varied by changing the magnetic field, while $\mathbf{s}$ can be tuned by applying an electric field in one layer. The form factor $F_{\mathbf{q}}^{\sigma} = \exp[-(g_m^\sigma)^{ab} q_a q_b \ell_B^2/4]$ depends on the band mass tensor in each layer g_m^σ [23] (we use Einstein's summation convention). The 2×2 unimodular matrix g_m^σ measures the mass anisotropy in layer σ which is induced, e.g., by tilting the magnetic field. In the isotropic case we have $g_m^\sigma = \mathbb{1}$, where $\mathbb{1}$ is the 2×2 identity matrix.

For small interlayer distances, $d \lesssim \ell_B$, the ground state of the bosonic $\nu = 2/3$ FQH bilayer is described by the Halperin (221) state [40], an incompressible fluid with total momentum $\mathbf{k} = \mathbf{0}$. At large values of d, the system transitions to two decoupled $\nu = 1/3$ states, each being a bosonic analog of the composite fermion Fermi liquid [41,42]. We are interested in probing the nonequilibrium behavior of the (221) system using a global quench of the system's Hamiltonian $H(g_m^\sigma, \mathbf{s})$ defined in Eq. (1). In our calculations we fix $d = 0.4\ell_B$. Initially the system is in the ground state $|\Psi_0\rangle$ of $H_0 \equiv H(g_m^{\uparrow,\downarrow} = \mathbb{1}, \mathbf{s} = \mathbf{0})$ in the (221) phase. At time $t = 0$, we suddenly modify the Hamiltonian $H_0 \to H'$, and let the system evolve according to the Schrödinger equation $|\Psi(t)\rangle = e^{-iH't}|\Psi_0\rangle$.

The sudden change of the Hamiltonian defines the quench, and we consider two protocols: (i) applying electric field in a single layer [Fig. 1(a)], which is equivalent to changing $\mathbf{s}$ from $\mathbf{0}$ to $\mathbf{s}' \neq \mathbf{0}$; and/or (ii) changing the mass tensor g_m^σ from $\mathbb{1}$ to $g_m^{\sigma\prime} \neq \mathbb{1}$ to add anisotropy in both layers [Fig. 1(b)], where $g_m^{\sigma\prime}$ is taken to be diagonal for simplicity. We find that the essential features of postquench dynamics are independent of precise values of $\mathbf{s}'$ and $g_m^{\sigma\prime}$ as long as the ground state of $H' \equiv H(g_m^\sigma = g_m^{\sigma\prime}, \mathbf{s} = \mathbf{s}')$ remains in the (221) phase, which we assume below.

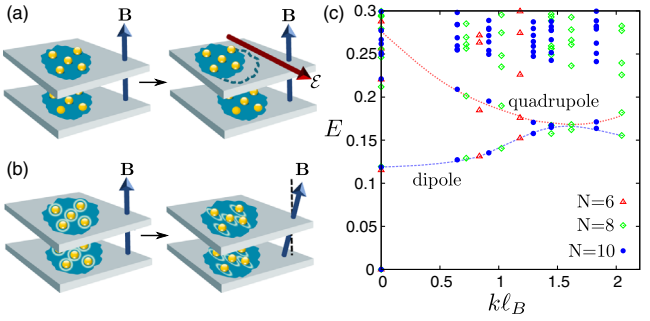

FIG. 1. (a) Instantaneous application of an electric field $\mathcal{E}$ in one layer induces dynamics in the relative displacement between FQH droplets in the two layers. (b) Instantaneous change of the mass tensors in both layers (or, equivalently, a sudden tilt of the magnetic field $\mathbf{B}$) induces dynamics in the intrinsic anisotropy [32], which describes the shape of flux-particle composites of the underlying FQH state. (c) Coulomb spectra of $N = 6$, 8, 10 bosons on the torus for $d = 0.4\ell_B$ showing the quadrupole and dipole collective modes. Dashed lines trace out these collective modes as a guide to the eye.

The key to understanding the dynamics lies in the excited states of $H(g_m^\sigma, \mathbf{s})$. A typical energy spectrum of the (221) system on the torus is shown in Fig. 1(c). The ground state is in the $\mathbf{k} = \mathbf{0}$ momentum sector, and there are two excitation modes above it. On the sphere, the upper mode starts from the total angular momentum $L = 2$ and hence is termed a quadrupole mode [18,19], while the lower mode starts from $L = 1$ and forms a dipole excitation. We note that the dispersion of these two modes is not sensitive to the precise values of g_m^σ and $\mathbf{s}$. In the language of field theory, the two modes are described using a degree of freedom that carries spin-2 and spin-1, respectively, in the long-wavelength limit. In the context of SMA, the long-wavelength limits of the quadrupole and dipole modes can be obtained by acting on the ground state with $\rho_{\mathbf{q}}^S = (\rho_{\mathbf{q}}^\uparrow + \rho_{\mathbf{q}}^\downarrow)/\sqrt{2}$ and $\rho_{\mathbf{q}}^{AS} = (\rho_{\mathbf{q}}^\uparrow - \rho_{\mathbf{q}}^\downarrow)/\sqrt{2}$, respectively [20,36,38]. As our quench protocols preserve translation symmetry, only eigenstates with $\mathbf{k} = \mathbf{0}$ are involved in the dynamics.

Electric-field quench.—Let us first consider the quench in which we apply an electric field instantaneously in one layer while keeping g_m^σ in both layers isotropic. For simplicity, we consider an electric field in the x direction, whose effect can be captured by changing the interlayer displacement $\mathbf{s}$ from (0,0) to $(s, 0)$, with $s \neq 0$ (the electric field also lifts the degeneracy of the LLL orbitals, but this effect is negligible for the system sizes we study). We compute the post-quench fidelity $F(t) = |\langle\Psi_0|\Psi(t)\rangle|$ to

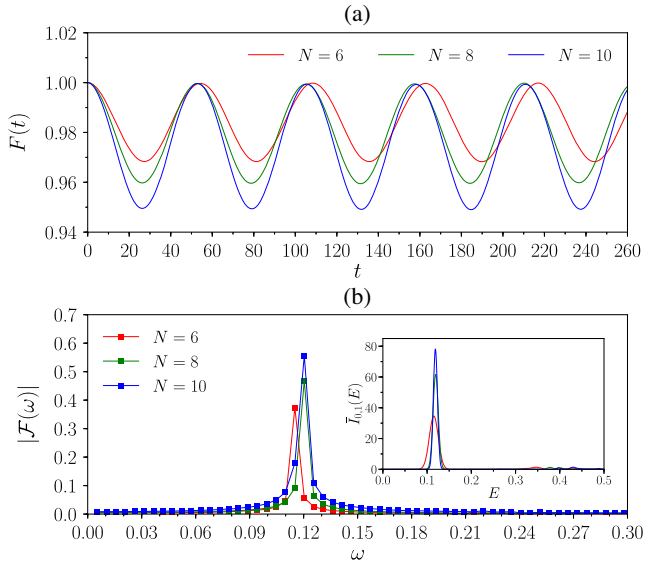

FIG. 2. (a) The fidelity $F(t)$ and (b) its discrete Fourier transform $|\mathcal{F}(\omega)|$ for the quench driven by tuning the interlayer displacement $\mathbf{s}$ from (0,0) to $(s,0)$ with $s = 0.1\ell_B$. The inset of (b) shows the normalized spectral function $\bar{I}_{0,1}(E) = I_{0,1}(E)/\int I_{0,1}(E)dE$ for isotropic systems with zero interlayer displacement. Markers in the main figure and curves in the inset with the same color refer to the same system size.

monitor the dynamics. We find that $F(t)$ oscillates regularly with a single dominant frequency, as shown in Fig. 2(a) for $s = 0.1\ell_B$, and this frequency is almost the same for different system sizes and other small s. To extract this frequency, we plot the discrete Fourier transform $|\mathcal{F}(\omega)|$ of $F(t)$ in Fig. 2(b). We see that $|\mathcal{F}(\omega)|$ has a sharply pronounced peak at $\omega \approx 0.12$ which is in excellent agreement with the energy of the spin-1 dipole mode in the long-wavelength limit [see Fig. 1(c)].

As shown in Fig. 1(c), the entire dipole mode lies below the continuum of the energy spectrum. This allows us to readily identify the coherent oscillations under the applied electric field with the dipole mode. This will not be the case with other types of quenches considered below. To unambiguously identify the modes excited by a quench, we construct appropriate spectral functions and locate their peaks. In the dipole case, we use the spectral function of an operator carrying spin-1 evaluated in the $\mathbf{k} = \mathbf{0}$ sector. A natural choice for such an operator is the $V_{0,1}$ generalized pseudopotential [72], adapted to the bilayer case, i.e., $\hat{V}_{0,1} = \sum_{\mathbf{q}} \bar{V}_{0,1}(\mathbf{q})$: $(\rho^{\uparrow}_{\mathbf{q}}\rho^{\downarrow}_{-\mathbf{q}} - \rho^{\downarrow}_{\mathbf{q}}\rho^{\uparrow}_{-\mathbf{q}})$: with $V_{0,1}(\mathbf{q}) \propto iq_x$. The corresponding spectral function $I_{0,1}(E)$ is

$$I_{0,1}(E) = \sum_j \delta(E - \epsilon_j + \epsilon_0)|\langle j|\hat{V}_{0,1}|0\rangle|^2, \qquad (2)$$

where ϵ_p is the energy of the eigenstate $|p\rangle$ of the general Hamiltonian $H(g^{\sigma}_m, \mathbf{s})$ defined in Eq. (1). Note that the bilayer $\hat{V}_{0,1}$ is defined to be antisymmetric with respect to the layer index because all layer-symmetric terms vanish for $V_{0,1}(\mathbf{q})$. As $\hat{V}_{0,1}$ couples the ground state with excited states with $L_z = 1$ (spin-1), the peaks in $I_{0,1}(E)$ correspond to spin-1 eigenstates. We show $I_{0,1}(E)$ in the inset of Fig. 2(b) for isotropic systems with $\mathbf{s} = \mathbf{0}$ (very similar data are obtained for weakly anisotropic systems with small $\mathbf{s}$). Indeed, $I_{0,1}(E)$ has a sharp peak at $E \approx 0.12$, agreeing with the lowest-excited state in the $\mathbf{k} = \mathbf{0}$ sector. This further confirms that the long-wavelength limit of the spin-1 dipole mode governs the electric-field-driven quench dynamics.

Mass anisotropy quench.—We now turn to the quench driven by mass anisotropy. In this case, we drive the quench by keeping $\mathbf{s} = \mathbf{0}$ and changing the mass tensors g^{σ}_m in both layers from $\mathbb{1}$ to $\mathrm{diag}\{\alpha, 1/\alpha\}$ with $\alpha > 1$ at $t = 0$. In single-layer FQH systems, the quench dynamics driven by mass anisotropy is dominated by a single spin-2 degree of freedom, which was identified with the long-wavelength limit of the GMP mode [32]. Since bilayer FQH systems have multiple neutral excitations, we expect the dynamics of bilayer mass-anisotropy quench to be richer than the single-layer case.

Like in the electric-field quench, we first study the fidelity $F(t)$, shown in Fig. 3(a) for $\alpha = 1.3$. It is clear that $F(t)$ now oscillates with multiple frequencies. To extract the dominant frequencies we plot the discrete Fourier transform $|\mathcal{F}(\omega)|$ of $F(t)$ in Fig. 3(b). Indeed we observe several pronounced peaks that are insensitive to small variations in α. As changing the mass tensor leads to quadrupolar (spin-2) deformations of FQH droplets [32,72], we expect these dominant frequencies to correspond to spin-2 degrees of freedom in the $\mathbf{k} = \mathbf{0}$ sector of H'. To substantiate this quantitatively, we utilize the spectral function of a spin-2 operator in the $\mathbf{k} = \mathbf{0}$ sector. We choose the operator $\hat{V}_{0,2} = \sum_{\mathbf{q}} \bar{V}_{0,2}(\mathbf{q})$: $\rho^S_{\mathbf{q}}\rho^S_{-\mathbf{q}}$: with $V_{0,2}(\mathbf{q}) \propto q_x^2 - q_y^2$, which is the bilayer generalization of the $V_{0,2}$ generalized pseudopotential [72]. Its spectral function $I_{0,2}(E)$ is defined analogously to Eq. (2). As shown in Fig. 3(c), the positions of peaks in $I_{0,2}$ indeed match those in $|\mathcal{F}(\omega)|$. Thus all dominant frequencies in the postquench dynamics correspond to spin-2 eigenstates in the $\mathbf{k} = \mathbf{0}$ sector of H'.

What is the physical interpretation of the multiple spin-2 states observed in the dynamics? On the one hand, the long-wavelength limit of the quadrupole mode, i.e., the bilayer spin-2 graviton, should definitely contribute. As suggested by the exact energy spectrum in Fig. 1(c), the quadrupole mode approaches the energy $E \approx 0.25$–0.3 in the long-wavelength limit, and there are indeed corresponding sharp peaks in $|\mathcal{F}(\omega)|$ [cyan-shaded area in Fig. 3(b)]. The splitting of these peaks is due to "fragmentation" of the spin-2 graviton mode into several states in finite systems, a feature which is also observed in single-layer systems [32]. On the other hand, although the long-wavelength limit of the spin-1 dipole mode cannot couple to the quench, a suitable combination of two spin-1 states can be excited by it. Two spin-1 states can form a bound state with spin-2,

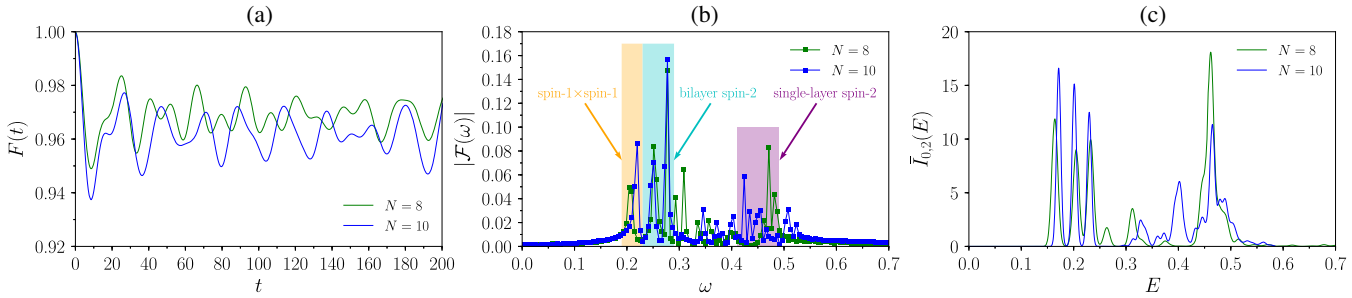

FIG. 3. (a) The fidelity $F(t)$ for the quench driven by tuning the mass tensors in both layers from $\mathbb{1}$ to $\mathrm{diag}\{\alpha, 1/\alpha\}$ with $\alpha = 1.3$ for $d = 0.4\ell_B$. (b) The discrete Fourier transform $|\mathcal{F}(\omega)|$ of $F(t)$. The three types of dominant frequencies, i.e., the combination of two spin-1 modes (orange), the bilayer spin-2 graviton (cyan), and the spin-2 state in a single layer (purple), are indicated by shaded areas and arrows. (c) The normalized spectral function $\bar{I}_{0,2}(E) = I_{0,2}(E)/\int I_{0,2}(E)dE$ for isotropic systems with zero interlayer displacement (very similar data are obtained for weakly anisotropic systems with small $\mathbf{s}$).

whose energy is slightly reduced from twice the spin-1 energy. The spectrum shown in Fig. 1(c) and results of the electric-field quench suggest that the dipole mode goes to $E \approx 0.12$ in the long-wavelength limit, thus a bound state of two dipoles, with energy $E < 0.24$, could appear in the postquench dynamics. Remarkably, we indeed observe a sharp peak at that energy in $|\mathcal{F}(\omega)|$ [orange-shaded area in Fig. 3(b)].

Curiously, in addition to the bilayer spin-2 graviton and the bound state of two spin-1's, we also see peaks in $|\mathcal{F}(\omega)|$ at a much higher frequency $\omega \approx 0.45$–0.5 [purple shaded area in Fig. 3(b)]. In principle, higher multiples of the elementary spin-1 and spin-2 modes may be expected to appear in the dynamics, but their contribution to the spectral function is expected to be significantly reduced. Moreover, we find these higher-frequency peaks become sharper and move to higher frequencies with increasing d when the two layers are progressively more decoupled [42]. Hence, we identify this spin-2 excitation with that of a single-layer $\nu = 1/3$ bosonic system.

Effective field theory.—Similar to the single-layer case, the bilayer spin-2 graviton can be described by the bimetric theory [24]. Here we outline the effective theory describing the new collective spin-1 mode. The theory is a spin-1 counterpart of the bimetric theory with a vector degree of freedom $\boldsymbol{v} = (v_x, v_y)$ that quantifies relative displacement of layers, described by the Lagrangian

$$\mathscr{L} = -\varepsilon^{ij} v_i \dot{v}_j - M|\boldsymbol{v}|^2 + \mathcal{E}_i^- v_i, \tag{3}$$

where $\mathcal{E}_i^-$ is the difference between electric fields applied to the layers and M determines the gap of the spin-1 mode. The quench is simulated by suddenly switching on $\mathcal{E}_i^-$ at $t = 0$ and solving classical equations of motion [32,73]. Assuming that the quench is along the x direction, i.e., $\mathcal{E}_y^- = 0$, the equations of motion stemming from Eq. (3) are single harmonics

$$v_x(t) = A[1 - \cos(Mt)], \qquad v_y(t) = A\sin(Mt), \tag{4}$$

where the amplitude of oscillations is determined by the quench strength, $A = \mathcal{E}_x^-/(2M)$.

Dynamics of v_i coming from Eq. (4) can then be compared to a numerical simulation, where $v_i(t)$ is determined by a brute force search over a large set of precomputed trial (221) states $|\Psi_{\mathrm{trial}}(\mathbf{s})\rangle$, i.e., the ground state of the Hamiltonian $H(g_m^{\uparrow,\downarrow} = \mathbb{1}, \mathbf{s})$. When the overlap $|\langle\Psi(t)|\Psi_{\mathrm{trial}}(\mathbf{s})\rangle|$ is maximized (and sufficiently close to unity), we expect $v_i(t) = s_i$. In Fig. 4, we show dynamics of v_i for various weak electric-field quench strengths and compare it to Eq. (4). Fitting the first oscillation in Fig. 4 against Eq. (4), we find a remarkable agreement between numerically exact dynamics and field-theory predictions up to moderate times. The frequency M returned by the fit matches the energy ≈ 0.12 of the $\mathbf{k} = \mathbf{0}$ spin-1 state, and the oscillation amplitude is given by $A = 2s$. With increasing quench strength or at longer times, we observe deviations from simple harmonic oscillations, which we believe is caused by effects like fragmentation of the long-wavelength limit of the dipole mode and the interaction between spin-1 states.

To describe the spin-2 bound state of the spin-1 modes we must include the interaction term, $\mathcal{L}_{\mathrm{int}} \propto |\boldsymbol{v}|^4$, into Eq. (3). It is then straightforward to show that $\langle v_i v_j \rangle$

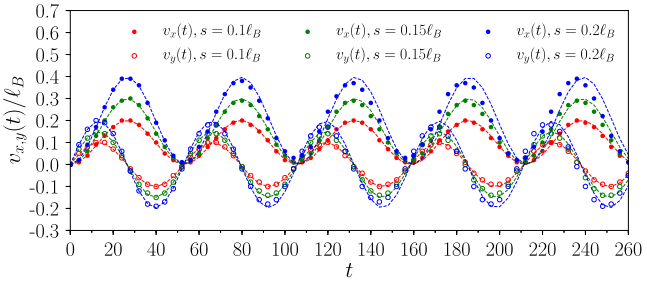

FIG. 4. Exact dynamics of the relative displacement $\boldsymbol{v}$ in the x (dots) and y directions (circles) for $N = 10$ bosons after quenches driven by tuning the interlayer displacement $\mathbf{s}$ from (0,0) to $(s, 0)$ with $s = 0.1\ell_B$, $0.15\ell_B$, $0.2\ell_B$. The dashed curves are fits to Eq. (4).

behaves as a spin-2 mode and responds to the geometric quench, leading to an extra peak in Fig. 3(b) [42].

Discussion.—In this work, we explored the quench dynamics of collective modes in bilayer $\nu = 2/3$ systems of bosons. We proposed and numerically simulated two quench protocols which excite neutral degrees of freedom in the system. The quench driven by an electric field applied in one layer induces oscillations of the long-wavelength limit of the spin-1 dipole collective mode. More interestingly, the quench driven by mass anisotropy not only activates the spin-2 quadrupole mode but also single-layer spin-2 excitation and a combination of two spin-1 dipole modes. While in this Letter we presented results for systems of bosons, all of our conclusions also hold for FQH systems of fermions.

Direct access to the spin-1 mode in the spectrum of bilayer states suggests a variety of new problems related to the geometric aspects of FQH and exact calculations of correlation functions [23,74–80]. Namely, which correlations functions are sensitive to the mode, and can any of them be computed with the help of existing methods?

Our quench protocols provide an opportunity to experimentally measure the collective modes of FQH states at long wavelengths in a way that complements the inelastic light scattering [28–31] and current noise measurements [81]. In fact, the quench protocols proposed in this work, in particular the counterflow electric field, can be implemented with the existing technology. The main challenge would be measuring the dynamics on short timescales in solid-state materials, which could be naturally resolved in other platforms, e.g., cold atoms in optical lattices forming a fractional Chern insulator [82–84]. Our results are also of direct relevance to more complex FQH systems with non-Abelian topological order, which also host multiple types of neutral excitations [85,86]. It would be interesting to design quench protocols and effective theories to probe different collective modes at long wavelengths as well as the combination (or interaction) between them.

Z. L. is supported by the National Natural Science Foundation of China through Grant No. 11974014 and by the National Key Research and Development Program of China through Grant No. 2020YFA0309200. A. C. B. acknowledges the Science and Engineering Research Board (SERB) of the Department of Science and Technology (DST) for financial support through the Start-up Grant SRG/2020/000154. A. C. B. and Z. P. thank the Royal Society International Exchanges Award IES\R2 \202052 for funding support. Some of the numerical calculations reported in this work were carried out on the Nandadevi supercomputer, which is maintained and supported by the Institute of Mathematical Science's High Performance Computing center. Z. P. acknowledges support by the Leverhulme Trust Research Leadership Award RL-2019-015 and by EPSRC grant EP/R020612/1. Statement of compliance with EPSRC policy framework on research data: This publication is theoretical work that does not require supporting research data. A. G. is supported by the Brown University.

[1] P. W. Anderson, *Concepts in Solids: Lectures on the Theory of Solids* (World Scientific, Singapore, 1997), Vol. 58.
[2] R. Feynman, *Statistical Mechanics: A Set of Lectures*, Advanced Books Classics (Avalon Publishing, New York, 1998).
[3] B. I. Lundqvist, Single-particle spectrum of the degenerate electron gas, Phys. Kondens. Mater. **6**, 206 (1967).
[4] A. W. Overhauser, Simplified theory of electron correlations in metals, Phys. Rev. B **3**, 1888 (1971).
[5] I. Affleck, T. Kennedy, E. H. Lieb, and H. Tasaki, Valence bond ground states in isotropic quantum antiferromagnets, Commun. Math. Phys. **115**, 477 (1988).
[6] D. P. Arovas, A. Auerbach, and F. D. M. Haldane, Extended Heisenberg Models of Antiferromagnetism: Analogies to the Fractional Quantum Hall Effect, Phys. Rev. Lett. **60**, 531 (1988).
[7] M. Takahashi, Excitation spectra of $S = 1$ antiferromagnetic chains, Phys. Rev. B **50**, 3045 (1994).
[8] E. S. Sorensen and I. Affleck, $s(k)$ for haldane-gap antiferromagnets: Large-scale numerical results versus field theory and experiment, Phys. Rev. B **49**, 13235 (1994).
[9] D. P. Arovas, Two exact excited states for the $S = 1$ AKLT chain, Phys. Lett. A **137**, 431 (1989).
[10] R. Thomale, S. Rachel, B. A. Bernevig, and D. P. Arovas, Entanglement analysis of isotropic spin-1 chains, J. Stat. Mech. (2015) P07017.
[11] S. Moudgalya, N. Regnault, and B. A. Bernevig, Entanglement of exact excited states of Affleck-Kennedy-Lieb-Tasaki models: Exact results, many-body scars, and violation of the strong eigenstate thermalization hypothesis, Phys. Rev. B **98**, 235156 (2018).
[12] J. Haegeman, B. Pirvu, D. J. Weir, J. I. Cirac, T. J. Osborne, H. Verschelde, and F. Verstraete, Variational matrix product ansatz for dispersion relations, Phys. Rev. B **85**, 100408(R) (2012).
[13] L. Vanderstraeten, J. Haegeman, and F. Verstraete, Simulating excitation spectra with projected entangled-pair states, Phys. Rev. B **99**, 165121 (2019).
[14] D. C. Tsui, H. L. Stormer, and A. C. Gossard, Two-Dimensional Magnetotransport in the Extreme Quantum Limit, Phys. Rev. Lett. **48**, 1559 (1982).
[15] R. B. Laughlin, Anomalous Quantum Hall Effect: An Incompressible Quantum Fluid with Fractionally Charged Excitations, Phys. Rev. Lett. **50**, 1395 (1983).
[16] D. Arovas, J. R. Schrieffer, and F. Wilczek, Fractional Statistics and the Quantum Hall Effect, Phys. Rev. Lett. **53**, 722 (1984).
[17] G. Moore and N. Read, Nonabelions in the fractional quantum Hall effect, Nucl. Phys. **B360**, 362 (1991).
[18] S. M. Girvin, A. H. MacDonald, and P. M. Platzman, Collective-Excitation Gap in the Fractional Quantum Hall Effect, Phys. Rev. Lett. **54**, 581 (1985).

[19] S. M. Girvin, A. H. MacDonald, and P. M. Platzman, Magneto-roton theory of collective excitations in the fractional quantum Hall effect, Phys. Rev. B **33**, 2481 (1986).

[20] S. R. Renn and B. W. Roberts, Magnetorotons and the fractional quantum Hall effect in double-quantum-well systems, Phys. Rev. B **48**, 10926 (1993).

[21] B. Yang, Z.-X. Hu, Z. Papić, and F. D. M. Haldane, Model Wave Functions for the Collective Modes and the Magneto-roton Theory of the Fractional Quantum Hall Effect, Phys. Rev. Lett. **108**, 256807 (2012).

[22] C. Repellin, T. Neupert, Z. Papić, and N. Regnault, Single-mode approximation for fractional Chern insulators and the fractional quantum Hall effect on the torus, Phys. Rev. B **90**, 045114 (2014).

[23] F. D. M. Haldane, Geometrical Description of the Fractional Quantum Hall Effect, Phys. Rev. Lett. **107**, 116801 (2011).

[24] A. Gromov and D. T. Son, Bimetric Theory of Fractional Quantum Hall States, Phys. Rev. X **7**, 041032 (2017).

[25] D. X. Nguyen, A. Gromov, and D. T. Son, Fractional quantum Hall systems near nematicity: Bimetric theory, composite fermions, and Dirac brackets, Phys. Rev. B **97**, 195103 (2018).

[26] S. Golkar, D. X. Nguyen, and D. T. Son, Spectral sum rules and magneto-roton as emergent graviton in fractional quantum Hall effect, J. High Energy Phys. 01 (2016) 021.

[27] A. Gromov, S. D. Geraedts, and B. Bradlyn, Investigating Anisotropic Quantum Hall States with Bimetric Geometry, Phys. Rev. Lett. **119**, 146602 (2017).

[28] A. Pinczuk, B. S. Dennis, L. N. Pfeiffer, and K. West, Observation of Collective Excitations in the Fractional Quantum Hall Effect, Phys. Rev. Lett. **70**, 3983 (1993).

[29] P. M. Platzman and S. He, Resonant raman scattering from magneto rotons in the fractional quantum Hall liquid, Phys. Scr. **T66**, 167 (1996).

[30] M. Kang, A. Pinczuk, B. S. Dennis, L. N. Pfeiffer, and K. W. West, Observation of Multiple Magnetorotons in the Fractional Quantum Hall Effect, Phys. Rev. Lett. **86**, 2637 (2001).

[31] I. V. Kukushkin, J. H. Smet, V. W. Scarola, V. Umansky, and K. von Klitzing, Dispersion of the excitations of fractional quantum Hall states, Science **324**, 1044 (2009).

[32] Z. Liu, A. Gromov, and Z. Papić, Geometric quench and nonequilibrium dynamics of fractional quantum Hall states, Phys. Rev. B **98**, 155140 (2018).

[33] M. F. Lapa, A. Gromov, and T. L. Hughes, Geometric quench in the fractional quantum Hall effect: Exact solution in quantum Hall matrix models and comparison with bimetric theory, Phys. Rev. B **99**, 075115 (2019).

[34] S.-F. Liou, F. D. M. Haldane, K. Yang, and E. H. Rezayi, Chiral Gravitons in Fractional Quantum Hall Liquids, Phys. Rev. Lett. **123**, 146801 (2019).

[35] S. M. Girvin and A. H. MacDonald, Multicomponent quantum Hall systems: The sum of their parts and more, in *Perspectives in Quantum Hall Effects* (Wiley-VCH Verlag GmbH, New York, 2007), pp. 161–224.

[36] A. H. MacDonald and S.-C. Zhang, Collective excitations in double-layer quantum Hall systems, Phys. Rev. B **49**, 17208 (1994).

[37] K. Moon, H. Mori, K. Yang, S. M. Girvin, A. H. MacDonald, L. Zheng, D. Yoshioka, and S.-C. Zhang, Spontaneous interlayer coherence in double-layer quantum Hall systems: Charged vortices and Kosterlitz-Thouless phase transitions, Phys. Rev. B **51**, 5138 (1995).

[38] K. Shizuya, Single-mode approximation and effective Chern-Simons theories for quantum Hall systems, Int. J. Mod. Phys. B **17**, 5875 (2003).

[39] *The Quantum Hall Effect*, edited by S. M. G. Richard and E. Prange (Springer-Verlag, New York, 1987).

[40] B. I. Halperin, Theory of the quantized Hall conductance, Helv. Phys. Acta **56**, 75 (1983).

[41] B. I. Halperin, P. A. Lee, and N. Read, Theory of the half-filled Landau level, Phys. Rev. B **47**, 7312 (1993).

[42] See Supplemental Material at http://link.aps.org/supplemental/10.1103/PhysRevLett.126.076604 for (i) more numerical data of quench dynamics and collective modes in the Halperin (221) systems, (ii) evidence in favor of the state at large layer separation being a decoupled pair of composite Fermi liquid of bosons each at $\nu = 1/3$, and (iii) an effective theory for the bound state of two spin-1 degrees of freedom, which includes Refs. [15,18,19,21,40,43–71].

[43] J. K. Jain, Composite-Fermion Approach for the Fractional Quantum Hall Effect, Phys. Rev. Lett. **63**, 199 (1989).

[44] G. Dev and J. K. Jain, Band Structure of the Fractional Quantum Hall Effect, Phys. Rev. Lett. **69**, 2843 (1992).

[45] J. K. Jain and R. K. Kamilla, Composite fermions in the Hilbert space of the lowest electronic Landau level, Int. J. Mod. Phys. B **11**, 2621 (1997).

[46] J. K. Jain, *Composite Fermions* (Cambridge University Press, New York, 2007).

[47] A. C. Balram, A. Wójs, and J. K. Jain, State counting for excited bands of the fractional quantum Hall effect: Exclusion rules for bound excitons, Phys. Rev. B **88**, 205312 (2013).

[48] F. D. M. Haldane, Fractional Quantization of the Hall effect: A Hierarchy of Incompressible Quantum Fluid States, Phys. Rev. Lett. **51**, 605 (1983).

[49] J. K. Jain and R. K. Kamilla, Quantitative study of large composite-fermion systems, Phys. Rev. B **55**, R4895 (1997).

[50] G. Möller and S. H. Simon, Composite fermions in a negative effective magnetic field: A Monte Carlo study, Phys. Rev. B **72**, 045344 (2005).

[51] S. C. Davenport and S. H. Simon, Spinful composite fermions in a negative effective field, Phys. Rev. B **85**, 245303 (2012).

[52] A. C. Balram, C. Töke, A. Wójs, and J. K. Jain, Fractional quantum Hall effect in graphene: Quantitative comparison between theory and experiment, Phys. Rev. B **92**, 075410 (2015).

[53] X. G. Wu, G. Dev, and J. K. Jain, Mixed-Spin Incompressible States in the Fractional Quantum Hall Effect, Phys. Rev. Lett. **71**, 153 (1993).

[54] K. Park and J. K. Jain, Phase Diagram of the Spin Polarization of Composite Fermions and a New Effective Mass, Phys. Rev. Lett. **80**, 4237 (1998).

[55] Y. Liu, S. Hasdemir, A. Wójs, J. K. Jain, L. N. Pfeiffer, K. W. West, K. W. Baldwin, and M. Shayegan, Spin polarization of composite fermions and particle-hole symmetry breaking, Phys. Rev. B **90**, 085301 (2014).

[56] A. C. Balram, C. Töke, A. Wójs, and J. K. Jain, Phase diagram of fractional quantum Hall effect of composite

fermions in multicomponent systems, Phys. Rev. B **91**, 045109 (2015).
[57] A. C. Balram, C. Töke, A. Wójs, and J. K. Jain, Spontaneous polarization of composite fermions in the $n = 1$ Landau level of graphene, Phys. Rev. B **92**, 205120 (2015).
[58] A. C. Balram and J. K. Jain, Fermi wave vector for the partially spin-polarized composite-fermion Fermi sea, Phys. Rev. B **96**, 235102 (2017).
[59] V. W. Scarola and J. K. Jain, Phase diagram of bilayer composite fermion states, Phys. Rev. B **64**, 085313 (2001).
[60] W. N. Faugno, A. C. Balram, A. Wójs, and J. K. Jain, Theoretical phase diagram of two-component composite fermions in double-layer graphene, Phys. Rev. B **101**, 085412 (2020).
[61] A. C. Balram and J. K. Jain, Nature of composite fermions and the role of particle-hole symmetry: A microscopic account, Phys. Rev. B **93**, 235152 (2016).
[62] A. C. Balram and J. K. Jain, Exact results for model wave functions of anisotropic composite fermions in the fractional quantum Hall effect, Phys. Rev. B **93**, 075121 (2016).
[63] R. K. Kamilla, X. G. Wu, and J. K. Jain, Excitons of composite fermions, Phys. Rev. B **54**, 4873 (1996).
[64] R. K. Kamilla, X. G. Wu, and J. K. Jain, Composite Fermion Theory of Collective Excitations in Fractional Quantum Hall Effect, Phys. Rev. Lett. **76**, 1332 (1996).
[65] A. C. Balram and S. Pu, Positions of the magnetoroton minima in the fractional quantum Hall effect, Eur. Phys. J. B **90**, 124 (2017).
[66] R. Morf, N. d'Ambrumenil, and B. I. Halperin, Microscopic wave functions for the fractional quantized Hall states at $\nu = \frac{2}{5}$ and $\frac{2}{7}$, Phys. Rev. B **34**, 3037 (1986).
[67] K. Park and J. K. Jain, Two-Roton Bound State in the Fractional Quantum Hall Effect, Phys. Rev. Lett. **84**, 5576 (2000).
[68] E. Rezayi and N. Read, Fermi-Liquid-Like State in a Half-Filled Landau Level, Phys. Rev. Lett. **72**, 900 (1994).
[69] A. C. Balram, C. Tőke, and J. K. Jain, Luttinger Theorem for the Strongly Correlated Fermi Liquid of Composite Fermions, Phys. Rev. Lett. **115**, 186805 (2015).
[70] A. C. Balram, A non-Abelian parton state for the $\nu = 2 + 3/8$ fractional quantum Hall effect, arXiv:2010.08965.
[71] B. Yang and A. C. Balram, Elementary excitations in fractional quantum Hall effect from classical constraints, New J. Phys. **23**, 013001 (2021).
[72] B. Yang, Z.-X. Hu, C. H. Lee, and Z. Papić, Generalized Pseudopotentials for the Anisotropic Fractional Quantum Hall Effect, Phys. Rev. Lett. **118**, 146403 (2017).
[73] F. Franchini, A. Gromov, M. Kulkarni, and A. Trombettoni, Universal dynamics of a soliton after an interaction quench, J. Phys. A **48**, 28FT01 (2015).
[74] D. X. Nguyen, T. Can, and A. Gromov, Particle-Hole Duality in the Lowest Landau Level, Phys. Rev. Lett. **118**, 206602 (2017).
[75] A. Gromov, G. Y. Cho, Y. You, A. G. Abanov, and E. Fradkin, Framing Anomaly in the Effective Theory of the Fractional Quantum Hall Effect, Phys. Rev. Lett. **114**, 016805 (2015).
[76] A. G. Abanov and A. Gromov, Electromagnetic and gravitational responses of two-dimensional noninteracting electrons in a background magnetic field, Phys. Rev. B **90**, 014435 (2014).
[77] A. Gromov and A. G. Abanov, Density-Curvature Response and Gravitational Anomaly, Phys. Rev. Lett. **113**, 266802 (2014).
[78] M. R. Douglas and S. Klevtsov, Bergman kernel from path integral, Commun. Math. Phys. **293**, 205 (2010).
[79] F. Ferrari and S. Klevtsov, FQHE on curved backgrounds, free fields and large N, J. High Energy Phys. 12 (2014) 086.
[80] T. Can, M. Laskin, and P. Wiegmann, Fractional Quantum Hall Effect in a Curved Space: Gravitational Anomaly and Electromagnetic Response, Phys. Rev. Lett. **113**, 046803 (2014).
[81] Y. N. Joglekar, A. V. Balatsky, and A. H. MacDonald, Noise Spectroscopy and Interlayer Phase Coherence in Bilayer Quantum Hall Systems, Phys. Rev. Lett. **92**, 086803 (2004).
[82] S. A. Parameswaran, R. Roy, and S. L. Sondhi, Fractional quantum Hall physics in topological flat bands, C. R. Phys. **14**, 816 (2013).
[83] E. J. Bergholtz and Z. Liu, Topological flat band models and fractional Chern insulators, Int. J. Mod. Phys. B **27**, 1330017 (2013).
[84] T. Neupert, C. Chamon, T. Iadecola, L. H. Santos, and C. Mudry, Fractional (Chern and topological) insulators, Phys. Scr. **T164**, 014005 (2015).
[85] G. Möller, A. Wójs, and N. R. Cooper, Neutral Fermion Excitations in the Moore-Read State at Filling Factor $\nu = 5/2$, Phys. Rev. Lett. **107**, 036803 (2011).
[86] P. Bonderson, V. Gurarie, and C. Nayak, Plasma analogy and non-Abelian statistics for Ising-type quantum Hall states, Phys. Rev. B **83**, 075303 (2011).